福井大学 工学部 研究報告 第49巻 第1号 2001年3月
Mem. Fac. Eng. Fukui Univ., Vol. 49, No. 1 (March 2001)

A Simple Model for Cyclic Plasticity Based on Activation State of Slip Systems

Takamoto ITOH*, Masaya KAMEOKA and Yoichi OBATAYA***

(Received February 26, 2001)

This paper proposes a new simple model for cyclic incremental plasticity based on activation states of slip systems describing stable cyclic stress-strain relationship under nonproportional loading. In this model, the magnitude and the direction of incremental plastic strain are estimated by $(1+\alpha f_{NP})$ and $\boldsymbol{Q}$, respectively. Here, α is the constant related to the material dependence of additional hardening and f_{NP} the nonproportional factor expressing the severity of nonproportional loading. $\boldsymbol{Q}$ is a second-order tensor describing the activation states of slip systems in polycrystalline metals and is given by the calculation using a virtual specimen. The model was examined the applicability to the estimation of the stable cyclic stress-strain relationship in extensive nonproportional low cycle fatigue tests for Type 304 stainless steel and 6061 aluminum alloy. The simulated results showed that the model gave a satisfactory estimation of the stable cyclic stress-strain relationship under the complex nonproportional multiaxial loadings for different materials.

Key Words : Constitutive Equation, Nonproportional Straining, Slip Systems, Low Cycle Fatigue

1. Introduction

Nonproportional multiaxial low cycle fatigue (LCF) lives are drastically decreased by an additional hardening due to nonproportional loading, which depends on both material and strain history. So, to predict the stable cyclic stress response is very important for the estimation of LCF lives under nonproportional multiaxial loadings. In the cyclic plasticity models based on the kinematic or isotropic hardening rule, a lot of material constants are required to describe the stress-strain relationship. Then, the material constants must be determined by using many experimental data, which is not always a simple procedure.

Itoh *et al.* [1,2] proposed the nonproportional strain parameter for predicting LCF lives of Type 304 stainless steel and 6061 aluminum alloy. The parameter is expressed as,

$$\Delta\varepsilon_{NP} = (1+\alpha f_{NP})\,\Delta\varepsilon_1 \qquad (1)$$

where $\Delta\varepsilon_1$ is the maximum principle strain range under nonproportional straining, α the material constant which discriminates the material dependency of additional hardening and f_{NP} the nonproportional factor which expresses the severity of nonproportional loading. The term $(1+\alpha f_{NP})$ has a possibility to estimate quantitatively the additional hardening due to nonproportional loading[3,4].

On the other hand, since macroscopic deformations of metals have a connection with actions of slip systems, it is considered that the cyclic deformation is closely related with the activation behavior of slip systems under nonproportional multiaxial LCF. So, activation states of slip systems should be able to show the cyclic deformation under nonproportional loadings. In the multiple strata plasticity model proposed by Obataya *et al.* [5,6], a tensor $\boldsymbol{Q}$ is introduced to describe the activation states of slip systems in polycrystalline metals.

In this study, by combining the term $(1+\alpha f_{NP})$ and the tensor $\boldsymbol{Q}$, a new cyclic plasticity model for describing the stable cyclic stress-strain relationship under nonproportional multiaxial straining is developed. In this model, the magnitude and the direction of incremental plastic strain are estimated by $(1+\alpha f_{NP})$ and $\boldsymbol{Q}$, respectively.

* Dept. of Mechanical Engineering
** Mechanical Engineering Course, Graduate School of Engineering

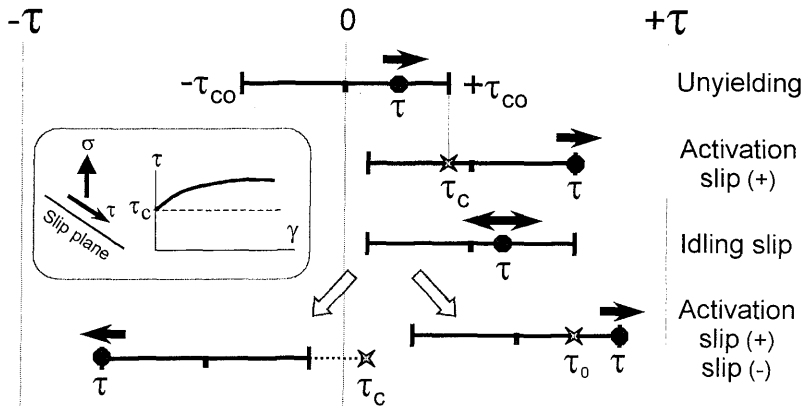

Fig.1 Activation state of slip system.

The present model was examined the applicability to the estimation of the stable cyclic stress-strain relationship in extensive nonproportional LCF tests for type 304 stainless steel and 6061 aluminum alloy.

2. Nonproportional LCF Parameter

2.1 Parameter for Additional Hardening

In the term of $(1+\alpha f_{NP})$, the value of α is defined as the ratio of stress amplitude under 90 degree out-of-phase loading (circular strain path in $\gamma/\sqrt{3}$-ε plot) to that under proportional loading. The 90 degrees out-of-phase loading shows the maximum additional hardening among all the nonproportional histories [1-3,7]. For 304 steel, the stress amplitude under 90 degrees out-of-phase loading was increased up to 90% in comparison with the proportional loading, so the value of α takes 0.9 [1]. For 6061 Al, it was 0.2 due to the small additional hardening [2].

The nonproportional factor which accounts for the severity of nonproportional strain is calculated from strain history, and is defined by

$$f_{NP}=\frac{\pi}{2T\varepsilon_{Imax}}\int_0^T\left(\left|\sin\xi(t)\right|\varepsilon_I(t)\right)dt \qquad (2)$$

where ε_I (t) and ξ(t) are the absolute value of maximum principal strain and the angle of maximum principal strain direction at any time t, respectively. T and ε_{Imax} are the time for a cycle and the maximum value of $\varepsilon_I(t)$ in a cycle. Detailed description of the nonproportional LCF parameter in Eq.1 is omitted here and the reader is referred to the previous paper [1,2] for details.

2.2 Parameter for Incremental Plastic Strain Direction

In the multiple strata plasticity model [5,6], the tensor $\boldsymbol{Q}$ is defined by calculation using a virtual polycrystalline specimen with a critical resolved shearing stress, τ_c, a plastic hardening exponent, n', and generalized Schmid factors in each slip system, μ. μ is expressed as,

$$\mu=\frac{1}{2}(\boldsymbol{a}\otimes\boldsymbol{b}+\boldsymbol{b}\otimes\boldsymbol{a}) \qquad (3)$$

where $\boldsymbol{a}$ is the unit vector normal to slip plane and $\boldsymbol{b}$ the unit vector of slip direction for each slip system. The resolved shear stress, τ, is given by

$$\tau=\mathrm{tr}(\mu\sigma) \qquad (4)$$

The hardening characteristic of activation state of slip systems was assumed to be given by following relationship between τ and the plastic shear strain, γ, in slip systems.

$$\tau=\tau_c\left(1+C\left|\gamma\right|^{n'}\right) \qquad (5)$$

where, C and n are the material constants. Then, we can obtain the incremental plastic shear strain as following equation,

$$d\gamma=\frac{1}{n'(C\,\tau_{co})^{1/n'}}\left(\left|\tau^r\right|-\tau_c^r\right)^{\frac{1}{n'}-1}d\tau \qquad (6)$$

In this equation, τ_{co} is the critical resolved shear stress at

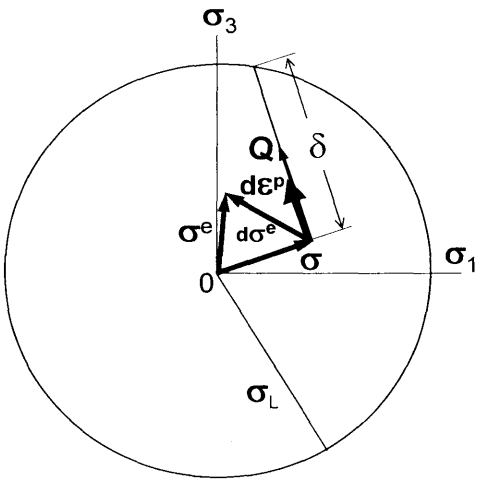

Fig.2 Illustration of model.

initial condition, and superior letter r denotes the activating slip systems' number. In the proposed model, τ_c for each slip system set a new value according to activation of slip system as the illustration in Fig.1.

Now, we can define the second-order tensor $\boldsymbol{Q}$, which express the activation state of slip systems and characterizes the direction of incremental plastic strain in the polycrystalline metal.

$$\boldsymbol{Q} = \frac{\sum_{r=1}^{M} \boldsymbol{\mu}^r \, d\gamma^r}{\sum_{r=1}^{M} |d\gamma^r|} \tag{7}$$

where M is the total number of activating slip systems employed in calculation with the virtual polycrystalline specimen.

3. Incremental Plasticity Model

When a thin-walled tube specimen is subjected to combined axial and torsional loading, the stress and strain state is expressed in terms of deviatoric vector planes. The definition of the axial-torsional subspace follows as an Ilyushin's five-dimensional deviatoric vector subspace and the stress vector is defines as

$$\boldsymbol{\sigma} = \sigma_1 \boldsymbol{n}_1 + \sigma_3 \boldsymbol{n}_3 \tag{8}$$

In this equation, σ_1 and σ_3 are the effective axial and shear stresses on Mises' base, respectively. $\boldsymbol{n}_1$ and $\boldsymbol{n}_3$ are the orthogonal base vectors in the stress space.

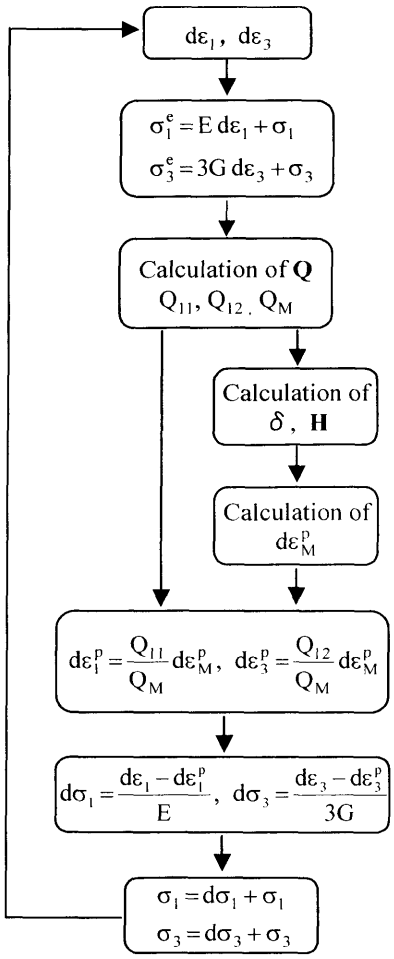

Fig. 3 Flowchart of analysis.

The strain vector is defined as

$$\boldsymbol{\varepsilon} = \varepsilon_1 \boldsymbol{n}_1 + \varepsilon_3 \boldsymbol{n}_3 \tag{9}$$

where ε_1 and ε_3 are the effective total axial and shear strains on Mises' base. The equivalent stress and the equivalent total strain are expressed by

$$\sigma_M = \sqrt{\sigma_1^{\,2} + \sigma_3^{\,2}}, \quad \varepsilon_M = \sqrt{\varepsilon_1^{\,2} + \varepsilon_3^{\,2}} \tag{10}$$

The incremental total strain, $d\boldsymbol{\varepsilon}$, is assumed to be decomposed into the elastic and incremental plastic strains, $d\boldsymbol{\varepsilon}^e$ and $d\boldsymbol{\varepsilon}^p$.

$$d\boldsymbol{\varepsilon} = d\boldsymbol{\varepsilon}^e + d\boldsymbol{\varepsilon}^p \tag{11}$$

where the incremental elastic strain components are given by

$$d\varepsilon_1^e = \frac{d\sigma_1}{E}, \qquad d\varepsilon_3^e = \frac{d\sigma_3}{3G} \tag{12}$$

In this equation, E and G are Young's and shear moduli, respectively.

Figure 2 illustrates σ, $d\varepsilon^p$ and Q and Figure 3 the flowchart of analysis in the model. As we put the incremental total strains, the stress vector, σ^e, is elastically calculated and is given by

$$\sigma^{e} = \sigma_1^e \boldsymbol{n}_1 + \sigma_3^e \boldsymbol{n}_3 \tag{13}$$

where

$$\sigma_1^e = E d\varepsilon_1 + \sigma_1, \quad \sigma_3^e = 3G d\varepsilon_3 + \sigma_3 \tag{14}$$

Now we put σ^e into σ in Eq.4 and then will obtain the tensor Q as schematically shown in Fig.2.

On the other hand, the strain hardening modulus for evaluation of the magnitude of incremental plastic strain is defined by

$$H = (1 + \alpha f_{NP}) K n \left(\frac{|\sigma_L - \delta|}{(1 + \alpha f_{NP})} \right)^{\frac{n-1}{n}} \tag{15}$$

where K and n are the cyclic hardening coefficient and exponent, assuming that the relationship between σ_M and ε^p_M can be express as

$$\sigma_M = K \left(\varepsilon_M^p \right)^n \tag{16}$$

σ_L is the radius of the limit surface which characterizes the cyclic hardening as well as K and n. Then, relationships between these parameters are

$$\begin{aligned} \sigma_L &= (1 + \alpha f_{NP}) K \\ n &= (1 + \alpha f_{NP}) n_0 \end{aligned} \tag{17}$$

where K and n_0 are set values obtained from tension-compression test. In Eq.15, δ is the distance between the stress point and the limit surface as shown in

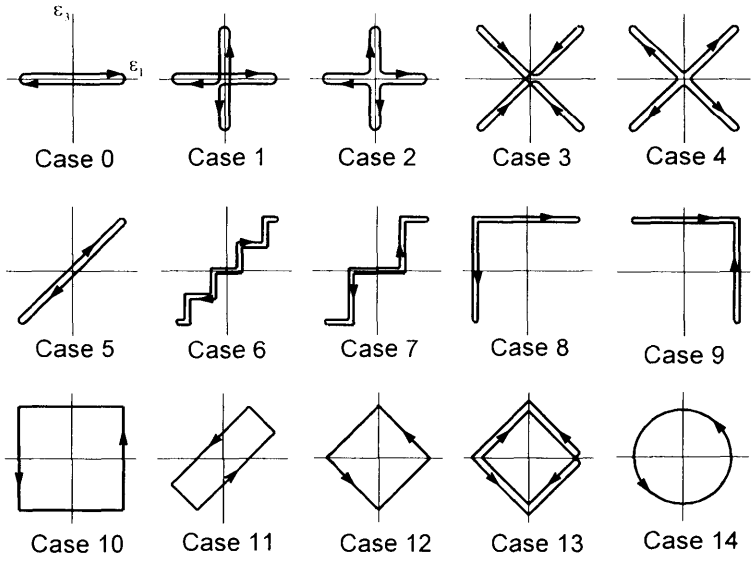

Fig.4 15 kinds of proportional and nonproportional strain paths.

Table 1 Material constants used in the analysis.

Material	304 steel	6061 Al
Young' modulus, E (GPa)	220	80
Shear modulus, G (GPa)	85	30
Cyclic hardening coefficent, K (MPa)	830	270
Cyclic hardening exponent, n [= n']	0.13	0.11
Critical resolved shear stress at initial state, τ_{c0} [=K/100] (MPa)	8.3	2.7
Material constant for additional hardening, α	0.8	0.4

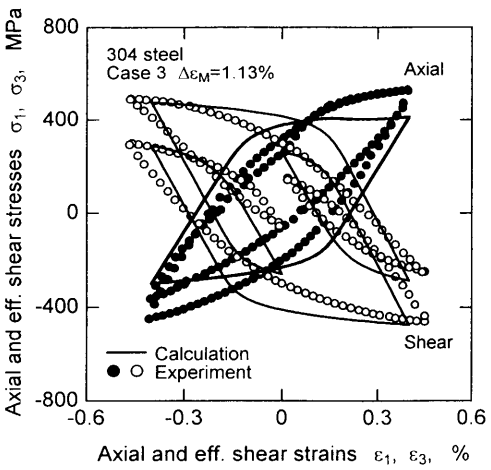

(a) 304 steel

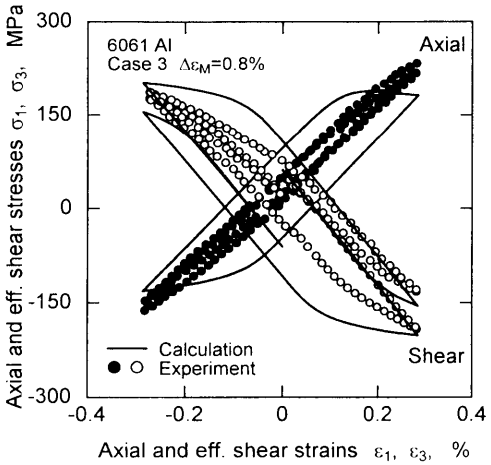

(b) 6061 Al alloy

Fig.5 Stable cyclic stress-strain relationship for Case 13.

Fig.2, and is given by

$$\delta = -\frac{\sigma_1 Q_{11} + \sigma_3 Q_{12}}{Q_M} + \sqrt{\frac{(\sigma_1 Q_{11} + \sigma_3 Q_{12})^2}{Q_M} + \sigma_L^2 - \sigma_M^2} \quad (18)$$

$$Q_M = \sqrt{Q_{11}^2 + \tfrac{1}{3} Q_{12}^2}$$

Then, we obtain the components of incremental plastic strains expressed by

$$d\varepsilon_1^p = \frac{Q_{11}}{Q_M} d\varepsilon_M^p, \quad d\varepsilon_3^p = \frac{Q_{12}}{Q_M} d\varepsilon_M^p \quad (19)$$

where

$$d\varepsilon_M^p = \sqrt{d\varepsilon_1^{\,2} + d\varepsilon_3^{\,2}} \frac{E}{E+H} \quad (20)$$

Finally, we can calculate the effective incremental

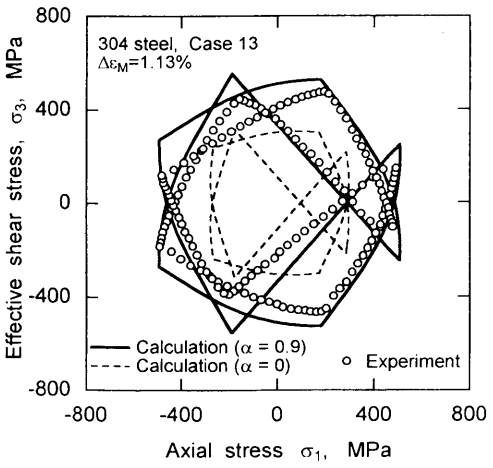

Fig.6 Stable cyclic stress response of 304 steel for Case 13.

stresses from the following equations.

$$d\sigma_1 = \frac{d\varepsilon_1 - d\varepsilon_1^p}{E}, \quad d\sigma_3 = \frac{d\varepsilon_3 - d\varepsilon_3^p}{3G} \quad (21)$$

4. Analytical Results and Discussion

The applicability to the estimation of the stable cyclic stress-strain relationship is examined using the nonproportional LCF data for Type 304 stainless steel and 6061 aluminum alloy. Mises' equivalent total strain controlled nonproportional LCF test were carried out using hollow cylinder specimens under 15 kinds of proportional and nonproportional strainings shown in Fig.4. Material constants used for the analysis are listed in Table 1. In virtual polycrystalline specimen[5,6], numbers of crystals and slip systems employed are 552 and 6624, respectively.

Figures 5 (a) and (b) shows the comparing the axial and shear stress-strain curves between calculation and experiment for Type 304 stainless steel and 6061 aluminum alloy in the tests of Case 3, respectively. The total strain ranges in these figures are 1.13% and 0.8% on Mises' base. The stresses in experiment in these figures are shown at $1/2N_f$. These figures show that the model developed in this study estimate an outline of the stress-strain curves in experiments. However, there are somewhat different between analysis and experiment along the strain path.

Figures 6 compares the stress response between calculation and experiment in Case 13 for Type 304 stainless

steel. In the figure, the broken line indicates the calculated result assuming the material constant α takes zero. The overall fitting of the stress-strain relationship between the prediction and experiment is good. In case of α=0, however, large difference of stress response between analysis and experiment can be seen, which shows a contribution of $(1+\alpha f_{NP})$ to the simulation is very large.

Figure 7 shows the comparison of effective stress ranges in all cases between calculation and experiment for two materials. These results show that the proposed model simulates the stable cyclic stress response and the stress ranges of all the tests within 20 % scatted band for different materials under nonproportional straining.

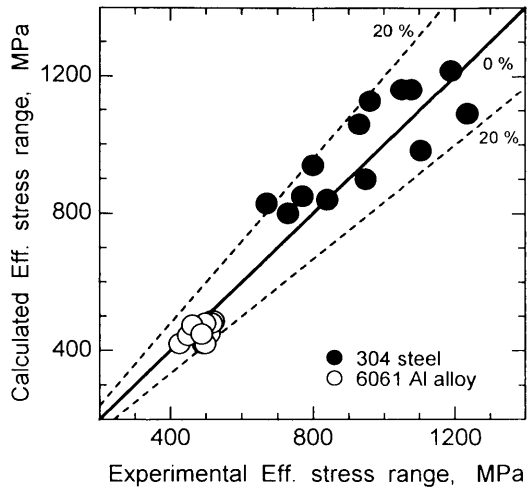

Fig.7 Comparison of the calculated and experimental effective stress ranges of all the tests for two materials.

5. Conclusion

The simulated results showed that the model gave a satisfactory estimation of the stable cyclic stress-strain relationship under the complex nonproportional multiaxial loadings for different materials, which is effective in the evaluation of nonproportional multiaxial low cycle fatigue damage.

References

[1] Itoh T., Sakane M., Ohnami M. and Socie D.F.: ASME JEMT. 117, 285 (1995).

[2] Itoh T., Sakane M., Ohnami M. and Socie D.F.: Multiaxial Fatigue & Fracture, E. Macha, W. Będkowsky and T. Łagda (Eds). ESIS-25. 41 (1999).

[3] Kida S., Itoh T., Sakane M., Ohnami M. and Socie D.F.: Fatigue Fract. Engng. Struct., 20, 1375 (1997).

[4] Itoh T., Chen X., Nakagawa T. and Sakane M.: ASME JEMT, 122, 1 (2000).

[5] Obataya Y., Jin Z.X., Okazaki A.: Proc. of AEPA'96, 375 (1996).

[6] Obataya Y. and Kato T.: Advances in Engineering Plasticity, Key Enginerring Materials, 177-180, 29 (2000).

[7] Socie D.F.: ASME JEMT, 109, 293 (1987).